

Quantification of ¹²³FP-CIT-SPECT in DLB

Confirmation of ¹²³I-FP-CIT-SPECT (ioflupane) quantification methods in Dementia with Lewy Body and other neurodegenerative disorders

Authors: Daniela D. Maltais,¹ Lennon G. Jordan,¹ Hoon-Ki Min,¹ Toji Miyagawa,² Scott A. Przybelski,³ Timothy G. Lesnick,³ Robert R. Reichard,⁴ Dennis W. Dickson,⁵ Melissa E. Murray,⁵ Kejal Kantarci,¹ Bradley F. Boeve,² and Val J. Lowe¹

Institutions: ¹Department of Radiology, Mayo Clinic, Rochester, MN; ²Department of Neurology, Mayo Clinic, Rochester, MN; ³Department of Health Sciences Research, Mayo Clinic, Rochester MN; ⁴Department of Anatomic Pathology, Mayo Clinic, Rochester MN; ⁵Department of Neuroscience, Mayo Clinic, Jacksonville, FL

Grant Support: U01-NS100620, P50-AG016574, P30-AG062677, GE Healthcare, Mayo Clinic Dorothy and Harry T. Mangurian Jr. Lewy Body Dementia Program, Deal Family Foundation, Little Family Foundation, and LBD Functional Genomics Program.

Corresponding author: Val J. Lowe, Department of Radiology, Mayo Clinic, Rochester, MN 55905. Email: vlowe@mayo.edu

First Author: Daniela D. Maltais, Post-baccalaureate scholar, Department of Radiology, Mayo Clinic, Rochester, MN 55905. Email: maltais.daniela@mayo.edu

Title: 15 words

Abstract: 305 words

Text: 2896

References: 39

Figures: 5

Tables: 5

ABSTRACT

Rationale: To conduct a retrospective study comparing three ^{123}I -FP-CIT-SPECT quantitative methods in patients with neurodegenerative syndromes as referenced to neuropathological findings.

Methods: ^{123}I -FP-CIT-SPECT and neuropathological findings among patients with neurodegenerative syndromes from the Mayo Alzheimer's Disease Research Center and Mayo Clinic Study of Aging were examined. Three ^{123}I -FP-CIT-SPECT quantitative assessment methods: MIMneuro (MIM Software Inc.), DaTQUANT (GE Healthcare), and manual region of interest (ROI) creation on an Advantage Workstation (GE Healthcare) were compared to neuropathological findings describing the presence or absence of Lewy body disease (LBD). Striatum to background ratios (SBRs) generated by DaTQUANT were compared to the calculated SBRs of the manual method and MIMneuro. The left and right SBRs for caudate, putamen and striatum were evaluated with the manual method. For DaTQUANT and MIMneuro the left, right, total and average SBRs and z-scores for whole striatum, caudate, putamen, anterior putamen, and posterior putamen were calculated.

Results: The cohort included 24 patients [20 (83%) male, aged 75.4 +/- 10.0 at death]. The antemortem clinical diagnoses were Alzheimer's disease dementia (ADem, N=6), probable dementia with Lewy bodies (pDLB, N=12), mixed ADem/pDLB (N=1), Parkinson's disease with mild cognitive impairment (N=2), corticobasal syndrome (N=1), idiopathic rapid eye movement sleep behavior disorder (iRBD) (N=1) and behavioral variant frontotemporal dementia (N=1). Seventeen (71%) had LBD pathology. All three ^{123}I -FP-CIT-SPECT quantitative methods had area under the receiver operating characteristics (AUROC) values above 0.93 and up to 1.000 ($p < 0.001$) and showed excellent discrimination between LBD and

non-LBD patients in each region assessed, $p < .001$. There was no significant difference between the accuracy of the regions in discriminating the two groups, with good discrimination for both caudate and putamen.

Conclusions: All three ^{123}I -FP-CIT-SPECT quantitative methods showed excellent discrimination between LBD and non-LBD patients in each region assessed, using both SBRs and z-scores.

Keywords: Dementia with Lewy Bodies; Lewy body disease; ^{123}I -FP-CIT-SPECT; ^{123}I -ioflupane; neuropathology

INTRODUCTION

Dementia with Lewy Bodies (DLB) is a neurodegenerative disorder clinically characterized by dementia associated with varying degrees of parkinsonism, cognitive fluctuations, recurrent visual hallucinations, and rapid eye movement (REM) sleep behavior disorder (iRBD)(1).

Probable DLB (pDLB), the dementia syndrome usually associated with underlying Lewy body Disease (LBD), is the second most common type of degenerative dementia in the older adult population following Alzheimer's Disease dementia (ADem) (2). The combination of degenerative motor and cognitive functions attribute to a higher mortality rate and greater use of resources in pDLB patients when compared to ADem patients with similar symptom severity (3,4). Many challenges relating to pDLB exist and have persisted for decades, particularly the difficulty in accurately predicting LBD pathology antemortem amongst those with dementia (5).

Challenges in diagnosis have arisen for three main reasons (5). First, there are few valid and reliable methods to assess core clinical features such as fluctuating cognition and visual hallucinations (5). Second, there are discrepancies between autopsy findings and the presentation of core clinical features. Third, the clinical and pathological overlap between pDLB and ADem, Parkinson's diseasevascular dementia, and frontotemporal lobar degeneration (FTLD) make these syndromes hard to discriminate; their common coexistence adds yet another layer of complexity, and makes the accuracy of reliance on clinical presentation alone imperfect (6). For these reasons, indicative biomarkers were proposed to support the clinical suspicion of pDLB based on core features alone (5).

^{123}I -FP-CIT SPECT, an indicative biomarker of pDLB, is currently one of the most widely used probes for imaging dopamine transporters (7,8). One study demonstrated a strong correlation between abnormal ^{123}I -FP-CIT-SPECT binding and LBD pathology (7), and other

studies suggest ^{123}I -FP-CIT-SPECT has 70-80% sensitivity for diagnosing probable clinical pDLB and over 80% specificity for excluding non-pDLB neurodegenerative syndromes (7). Currently, ^{123}I -FP-CIT-SPECT is often interpreted in clinical practice using only qualitative visual interpretation. However, there are several possible limitations when qualitative visual inspection is solely relied upon for interpretation (8). Subtle changes in the striatum or its specific sub-regions may be problematic on visual inspection and high reproducibility may be a challenge in longitudinal studies (8). For these reasons, automated, semi-automated and manual quantitative methods for ^{123}I -FP-CIT-SPECT could be helpful (8,9).

Ratios that compare the ^{123}I -FP-CIT-SPECT radiopharmaceutical uptake to a reference region of low dopamine transporter density are used in quantitative analyses (7). Some software programs may give options to manually position regions of interest (ROIs) on the images, however, this is time-consuming and leads to intra-rater and inter-rater variability (10).

Automated and semi-automated quantitative methods that have pre-defined ROIs in a normalized space are more time efficient, however, results may still be skewed in patients where low specific binding is expected if the pre-defined ROIs are not based on individual morphology (11). More success in the clinical diagnosis of dementia has been found when individual patient images were compared to a normative database that provided z-score maps, which compensate for age and gender effects (12).

Several quantification methods are available, including DaTQUANT (GE Healthcare) (9), MIMneuro (MIM Software Inc.) (13), and manual ROI creation on an Advantage Workstation (GE Healthcare) (7). In this study, we paired neuropathological findings and clinical data to investigate the comparative diagnostic accuracy of these quantification methods for predicting LBD vs non-LBD pathology.

MATERIALS AND METHODS

Participants

Participants with neurodegenerative syndromes from the Mayo Clinic Alzheimer's Disease Research Center and Mayo Clinic Study of Aging were examined. The inclusion criteria were as follows: 1. diagnosis of a neurodegenerative syndrome, 2. analyzable ^{123}I -FP-CIT SPECT, and 3. autopsy with neuropathologic examination. Published criteria enabled the consensus clinical diagnoses of a neurodegenerative syndrome, including ADem (14), pDLB (1), mixed ADem/pDLB, Parkinson's disease with mild cognitive impairment (15), corticobasal syndrome (16), FTLN (17), and (iRBD) (18). Polysomnography was used to confirm REM sleep without atonia, which is required for a diagnosis of definite iRBD. Mayo IRB approval was granted, and informed consent was given by the patient and/or proxies.

^{123}I -FP-CIT-SPECT Acquisitions

At least one hour before the injection of ^{123}I -Ioflupane, a 100 mg Lugols solution was given, and then the recommended ^{123}I -Ioflupane dose of 111 to 185 MBq (3 to 5 mCi) was administered slowly intravenously. ^{123}I -FP-CIT-SPECT was performed 3.2 ± 1.9 years before death in patients with pDLB and 2.4 ± 1.6 years before death in patients without pDLB. SPECT imaging occurred 3-6 hours post injection. GE D670/D630 SPECT systems with ultra-high-resolution fan beam collimators and an energy setting of 159 keV 20% window was used on all patients. Data was reconstructed using ordered subset expectation maximization method, and the planar images were pre-filtered using a Butterworth filter (power=10, cut-off= 0.6 cycles/cm), and no attenuation correction was used. For GE DaTQuant, we used projection images as input. Case

study SPECT images were co-registered with MRI using the VINCI program, provided by the Max Planck Institute (Munich, Germany).

Imaging Analysis

The presence or absence of LBD confirmed by neuropathological findings was compared against results from three ¹²³I-FP-CIT-SPECT quantitative methods: MIMneuro (MIM Software Inc.), DaTQUANT (GE Healthcare), and manual ROI creation on an Advantage Workstation (GE Healthcare). Selection of the best representative slide and placement of the ROIs was done in the manual method, and then the left and right striatum-to-background ratio (SBR) for caudate, putamen and striatum were calculated using the following formulas:

$$\frac{\textit{Right Caudate Mean}}{\textit{Average of the Left and Right Occipital Mean}} - 1 = \textit{SBR for Right Caudate,}$$

MIMneuro calculated the left and right striatum, caudate, putamen, anterior putamen, and posterior putamen z-scores. SBRs for the aforementioned regions were manually calculated using a similar formula to the one above. The left, right, and average z-scores and SBRs for the same regions used by MIMneuro were calculated by DaTQUANT. MIMneuro had three cases with co-registration error, and these were subsequently discarded. For the analysis, each left and right SBRs and z-scores were re-classified for ranking purposes; the lowest value was labeled as the minimum, the highest value as the maximum, and the average of the minimum and maximum labeled as the average.

Neuropathological Methods

Neuropathologists were blinded to the results of the ¹²³I-FP-CIT SPECT, and relied on previously published neuropathology assessments. Of these, the Braak Staging criteria (19,20), Consortium to Establish a Registry for Alzheimer's Disease scores (21), Thal A β phases (22), LBD pathologic criteria (1), and FTLN classification (23) were used.

Statistical Methods

Analyses of variance for continuous variables and a chi-squared test for categorical variables were used to test for differences with the characteristics amongst the three groups, LBD, LBD/AD and LBD Absent. Area under the receiver operating characteristics (AUROCs) were used to test for neuropathological group discrimination for the various semi-quantitative image analysis programs. Intraclass correlation coefficients (ICC) were used to assess the relationship between the image analysis programs and ROIs. Due to the differences in scales, the less stringent consistency approach was applied. Box-and-whisker plots displayed the distribution of ROIs (in z-score and SBR format) and their relation to neuropathological diagnosis. The reported cuff-off values on the boxplots were based upon the Youden method which maximizes the distance in relation to the identity line. Additional testing was performed using an ANOVA with contrast statements for pairwise comparisons. All of these analyses considered a p-value of <.05 as statistically significant.

RESULTS

Participants

Twenty-four patients met the inclusion criteria, of whom 11 had pathologic confirmation of LBD, 6 had a mixture of LBD and Alzheimer's Disease (AD) pathology, 7 had no LBD pathology (6 AD and 1 FTLN). A sensitivity analysis was run with the FTLN participant

excluded, and the results remained essentially the same. The demographic, clinical, pathologic, and ^{123}I -FP-CIT-SPECT characteristics of these patients are summarized in Supplemental Table 1. For these patients, the mean onset of cognitive decline was 65.9 ± 9.1 years. Twenty (83%) patients were male, and the mean age was 75.4 ± 10.0 years at death. The antemortem clinical diagnoses were ADem (N=6), pDLB (N=12), mixed ADem/pDLB (N=1), PD+MCI (N=2), CBS (N=1), iRBD (N=1) and FTLD (N=1). Patients came to autopsy at a mean age of 75.4 ± 10.0 years. Seventeen (71%) had LBD confirmed by neuropathology. Most (22/24) of the clinical diagnoses at the time of imaging were in concordance with the neuropathological findings. Clinical scales, such as the Boston Naming Test ($p=.10$) (24), Global Deterioration Scale ($p=.22$) (25) and Trail-Making Test Part A ($p=.14$) (26) were examined for differences and were not found to be statistically significant. MMSE ($p=.003$) (27), the Category Fluency Total ($p=.031$) (28) were found to be significant. Variables, such as apolipoprotein E4 (APOE4) ($p=.27$), time from scan date to death ($p=.60$), and education ($p=.33$) were not significant. On the other hand, sex ($p=.036$), age when the patient was scanned ($p=.029$) and age of patient death ($p=.028$) were found to be significant.

Imaging Analysis

The mean age ^{123}I -FP-CIT-SPECT was performed in all patients was 72.4 ± 9.5 years, and a mean of 3.0 ± 1.8 years represents the time between scan and death. Each possible ROI SBR and z-score generated by the three quantitative methods were compared against neuropathology data. The AUROC analysis demonstrated excellent group discrimination between LBD and Non-LBD cases for each program and each tested ROI (Figure 1). All AUROC values ranged from 0.93-1.000 ($p<.001$). Of note, the caudate minimum z-score achieved a 1.00 AUROC value or perfect

group separation. The SBRs and z-scores of all ROIs across all image analysis programs were ranked from greatest to least; the highest numerical AUROC values corresponded mainly to the minimum caudate, followed by the minimum striatum across all programs and scores. The 2x2 AUROC in Supplemental Figure 1 demonstrates the overlap found 1) in each program across the minimum striatum, minimum caudate and minimum putamen and 2) between programs.

Diagnoses given by radiologists derived from visual inspection alone were compared against neuropathology data. The AUROC (95% CI) analysis for this was: 0.971 (0.753, 0.997).

The ICC analysis of the image analysis programs showed strong associations: DaTQUANT SBR and Manual SBR for the caudate $r=0.913$, $p<.001$, putamen $r=0.898$, $p<.001$ and for the striatum $r=0.920$, $p<.001$. Similar trends were evident, although slightly lower, between the DaTQUANT z-score and MIMneuro z-score for the caudate $r=0.811$, $p<.001$, putamen $r=0.856$, $p<.001$, and for the striatum $r=0.855$, $p<.001$ (Figure 2). Across all image analysis programs and ROIs group separation of LBD versus no LBD was evident in box-and-whisker plots (Figure 3). Optimal cutoff values are delineated in red here, and numerically shown in Supplemental Table 2.

ANOVA models with contrast statements showed testing pairwise comparisons that the striatum, caudate and putamen quantified through DaTQUANT SBRs, DaTQUANT z-scores and manual were different in the following neuropathological categories: 1) AD versus LBD ($p<0.001$) and 2) AD versus LBD/AD ($p<0.001$). zMIM was also significantly different in the above categories ($p<0.05$). All three quantitative image analysis programs showed no differences between patients with LBD pathology and patients with mixed LBD/AD pathologies ($p<0.23$) (Supplemental Table 3).

Case Studies

Six cases highlighted the utility and limitation of ^{123}I -FP-CIT-SPECT (Figure 4). Case 1 was a 75-year-old female clinically diagnosed with ADem. ^{123}I -FP-CIT-SPECT was abnormal and neuropathology revealed diffuse dementia with Lewy body (DLBD) and AD with a Braak stage of VI. In this case, ^{123}I -FP-CIT-SPECT was able to detect profound abnormality in the midbrain despite a clinical presentation that resembled ADem. Case 2 was a 55-year-old male clinically diagnosed with ADem/pDLB. ^{123}I -FP-CIT-SPECT was normal, and neuropathology revealed no LBD, but AD with a Braak stage of VI. In this case, the dual clinical diagnosis disagreed with the single type of neuropathology found (AD). ^{123}I -FP-CIT-SPECT interpretation and neuropathology agreed, with high SBR values ranging from 2.56 to 2.74. Case 3 was a 63-year-old female clinically diagnosed with ADem. ^{123}I -FP-CIT-SPECT was normal and neuropathology revealed DLBD. While LBs were present in the substantia nigra as well as limbic and neocortical structures, the high SBR values (1.98 to 2.10) suggest that the degenerative changes in the nigrostriatal system were relatively mild and below the threshold of detection by ^{123}I -FP-CIT-SPECT imaging. Case 4 was a 59-year-old male clinically diagnosed with ADem. ^{123}I -FP-CIT-SPECT was normal and neuropathology revealed AD with a Braak stage of V. This was an example of a typical AD case; agreement existed between the clinical diagnosis, ^{123}I -FP-CIT SPECT, and neuropathology. Case 5 was a 74-year-old male clinically diagnosed with ADem. ^{123}I -FP-CIT-SPECT was normal and neuropathology revealed AD with amygdala restricted Lewy Bodies (ALB) and Braak stage VI. These “amygdala-only LBD” cases tend to occur in advanced AD, and are not viewed as reflecting typical LBD. Case 6 was a 77-year-old man clinically diagnosed with pDLB. ^{123}I -FP-CIT-SPECT was abnormal and neuropathology revealed DLBD, vascular dementia and pathological aging. ^{123}I -FP-CIT-SPECT

provided low SBR scores of 1.17 and 1.64, matching the clinical diagnosis of pDLB. MRI co-registered images that match the summary information in Table 1 and the neuropathological information in Table 2 are presented in Figure 4.

DISCUSSION

We examined the relationship between neuropathological findings and three semi-quantitative ^{123}I -FP-CIT-SPECT image analysis programs in a cohort of 24 patients. All three ^{123}I -FP-CIT-SPECT quantitative methods showed excellent discrimination between LBD and non-LBD patients in each region assessed using both SBRs and z-scores. Positive correlations were seen between programs and their respective z-scores in the caudate, putamen and striatum.

The combination of neuropathological findings (considered the gold standard) and clinical data has been shown to provide a more robust assessment of the role ^{123}I -FP-CIT-SPECT plays in the diagnosis of pDLB (29). Several studies reported the enhanced sensitivity and specificity of using ^{123}I -FP-CIT-SPECT over using clinical criteria alone, when both were paired with neuropathological data (30,31). In one such study, ^{123}I -FP-CIT SPECT's ability to indicate LBD had a sensitivity of 88% and a specificity of 100%, while clinical criteria alone had a 75% specificity and 42% sensitivity (31).

In our study, both visual inspection and semi-quantification assessment of ^{123}I -FP-CIT-SPECT showed good concordance with neuropathology results. Of the 17 confirmed LBD cases, visual inspection alone was able to detect abnormality in 16 (The single missed case is shown as Case 3 in Figure 4). However, the below cutoff minimum caudate z-score (derived from quantification)

corrected this false negative. Mixed DLBD/AD pathology was confirmed in 6 cases. In these 6 cases, four were clinically diagnosed with pDLB and two with ADem. Of these 6, one mixed DLBD/AD had a false negative and the other a true positive ^{123}I -FP-CIT SPECT. Among the six confirmed mixed DLBD/AD cases, the clinical diagnoses could be explained by any of the following: 1) one prominent pathology leads to the specific classifying symptomatology without the other pathology being clinically observed, 2) overlap of symptoms between pDLB and ADem cause confusion, or 3) time between last clinical evaluation and autopsy. Better characterization of these patients, whether they have mixed diseases or not, may be better refined with the use of multi-imaging (32). Sensitive tools, such as quantification programs used in serial imaging, could be particularly useful to assess specific signal changes over time that could add more confidence. Among the confirmed LBD cases, one case was clinically diagnosed as iRBD and two cases with Parkinson's Disease Dementia (PDD). ^{123}I -FP-CIT-SPECT identified these as abnormal and symptoms played a critical role in properly clinically characterizing these cases.

The utility of ^{123}I -FP-CIT-SPECT was highlighted two cases, one with ADem (case 1) and another with ADem/pDLB (case 2) as clinical diagnoses. In case 1, ^{123}I -FP-CIT-SPECT revealed absence of uptake in the left striatum indicative of LBD. In case 2, ^{123}I -FP-CIT-SPECT showed an intact striatum. These cases show that lower sensitivity in clinical diagnosis can be improved with ^{123}I -FP-CIT SPECT. As such, ^{123}I -FP-CIT-SPECT may be particularly helpful when atypical clinical features or diagnostic ambiguities are present (7). On the other hand, case 3 and case 5 highlighted the limitation of ^{123}I -FP-CIT-SPECT to assess LB in areas outside the striatum. Neuropathology revealed DLBD in case 3 and AD/ALB in case 5, while ^{123}I -FP-CIT-SPECT images of the striatum appeared relatively intact. The lower sensitivity in past ^{123}I -FP-

CIT-SPECT studies has been hypothesized to occur due to the presence of LBD pathology in the limbic +/- neocortical structures but less so in the nigrostriatal system in the early stages of disease (33). 18F-FE-PE2I, a novel DAT tracer, shows promise to discriminate between healthy controls and early Parkinson's Disease patients (34).

High diagnostic accuracy was found with visual inspection and all three quantification programs. Sample size, lack of blinding and experienced observers may have contributed to this finding. This contrasts with previous reports that have shown benefits of quantitative programs, such as improving diagnostic accuracy particularly amongst residents and less experienced physicians (8,35,36). Quantitative programs have been shown to capture subtle changes that may otherwise pass unobserved (8). It is noted that high accuracy was found for the manual semi-quantification method, viable alternative when commercial software programs are not available.

There were some limitations in this study. Difference based on attenuation correction, acquisition collimator, and image reconstruction methods were not assessed. Previous studies have reported 1) higher SBRs when attenuation correction, such as Chang and CTAC have been used (37) and 2) no difference in diagnostic impact between AC and non-AC images (38). Additionally, comparison between image analysis programs was restricted due to inconsistent data types in output files. Due to the absence of a normal database, the manual method could not generate z-scores which limited comparison of z-scores. From what could be examined there were no statistical differences between SBRs and z-scores, and this finding could be influenced by the number of participants, as well as by the matching process used in normative databases. Another

potential limitation of our study was the relatively small sample size. However, our findings were strengthened by the similarity of values across programs validated by autopsy results.

CONCLUSION

All three ^{123}I -FP-CIT-SPECT quantitative methods showed excellent discrimination between LBD and non-LBD patients in each region assessed, both through the use of SBRs and z-scores. Across all image analysis programs, the SBRs and z-scores for the minimum caudate and minimum striatum held the highest numerical AUROC value. Though ^{123}I -FP-CIT-SPECT does have a high diagnostic value (as shown here and in the literature), combining this with clinical and neuropsychological data is still important (33,39).

ACKNOWLEDGMENTS

Supported by National Institutes of Health (U01-NS100620 to KK and BFB, P50-AG016574 to BFB), GE Healthcare (BFB and VJL), Mayo Clinic Dorothy and Harry T. Mangurian Jr. Lewy Body Dementia Program, Deal Family Foundation, the Little Family Foundation, and the Lewy Body Dementia Functional Genomics Program.

Key Points:

Question: Which ^{123}I -FP-CIT-SPECT quantification method, ROI and score type can best discriminate between LBD and non-LBD patients when paired with neuropathological confirmation?

Findings: Three ^{123}I -FP-CIT-SPECT quantitative assessment methods: MIMneuro (MIM Software Inc.), DaTQUANT (GE Healthcare), and manual region of interest (ROI) creation on an Advantage Workstation (GE Healthcare) were compared to neuropathological findings describing the presence or absence of Lewy body disease (LBD). Using both SBRs and z-scores, all three quantitative methods showed excellent discrimination between LBD and non-LBD patients in each region assessed.

Implications for patient care: Quantitative image analysis programs studied here highlight 1) the utility of ^{123}I -FP-CIT-SPECT to support clinical diagnosis, especially for patients with a complicated presentation and 2) the potential research scope of quantification when compared to prior reliance on visual inspection alone.

REFERENCES

1. McKeith IG, Boeve BF, Dickson DW, et al. Diagnosis and management of dementia with Lewy bodies: fourth consensus report of the DLB Consortium. *Neurology*. 2017;89:88-100.
2. Zupancic M, Mahajan A, Handa K. Dementia with Lewy bodies: diagnosis and management for primary care providers. *Prim Care Companion CNS Disord*. 2011;13. PCC.11r01190.
3. Williams MM, Xiong CJ, Morris JC, Galvin JE. Survival and mortality differences between dementia with Lewy bodies vs Alzheimer disease. *Neurology*. 2006;67:1935-1941.
4. Bostrom F, Jonsson L, Minthon L, Londos E. Patients with Lewy body dementia use more resources than those with Alzheimer's disease *Int J Geriatr Psychiatry*. 2007;22:713-719.
5. McKeith IG, O'Brien JT, Walker Z, et al. Sensitivity and specificity of dopamine transporter imaging with ¹²³I-FP-CIT-SPECT in dementia with Lewy bodies: a phase III, multicentre study. *Lancet Neurol*. 2007;6:305-313.
6. Vlaar AM, de Nijs T, Kessels AG, et al. Diagnostic value of ¹²³I-ioflupane and ¹²³I-iodobenzamide SPECT scans in 248 patients with parkinsonian syndromes. *Eur Neurol*. 2008;59:258-266.
7. Jung Y, Jordan LG, Lowe VJ, et al. Clinicopathological and ¹²³I-FP-CIT-SPECT correlations in patients with dementia. *Ann Clin Transl Neurol*. 2018;5:376-381.
8. Augimeri A, Cherubini A, Cascini GL, et al. CADA-computer-aided DaTSCAN analysis. *EJNMMI Phys*. 2016;3. doi: 10.1186/s40658-016-0140-9.
9. Shimizu S, Namioka N, Hirose D, et al. Comparison of diagnostic utility of semi-quantitative analysis for DaT-SPECT for distinguishing DLB from AD. *J Neurol Sci*. 2017;377:50-54.
10. Badiavas K, Molyvda E, Iakovou I, Tsolaki M, Psarrakos K, Karatzas N. SPECT imaging evaluation in movement disorders: far beyond visual assessment. *Eur J Nucl Med Mol Imaging*. 2011;38:764-773.
11. Darcourt J, Booij J, Tatsch K, et al. EANM procedure guidelines for brain neurotransmission SPECT using (¹²³)I-labelled dopamine transporter ligands, version 2. *Eur J Nucl Med Mol Imaging*. 2010;37:443-450.
12. Minoshima S, Frey KA, Koeppe RA, Foster NL, Kuhl DE. A diagnostic approach in Alzheimer's disease using three-dimensional stereotactic surface projections of fluorine-18-FDG PET. *J Nucl Med*. 1995;36:1238-1248.

13. Partovi S, Yuh R, Pirozzi S, et al. Diagnostic performance of an automated analysis software for the diagnosis of Alzheimer's dementia with 18F-FDG-PET. *Am J Nucl Med Mol Imaging*. 2017;7:12-23.
14. McKhann GM, Knopman DS, Chertkow H, et al. The diagnosis of dementia due to Alzheimer's disease: recommendations from the National Institute on Aging-Alzheimer's Association workgroups on diagnostic guidelines for Alzheimer's disease. *Alzheimers Dement*. 2011;7:263-269.
15. Litvan I, Goldman JG, Tröster AI, et al. Diagnostic criteria for mild cognitive impairment in Parkinson's disease: Movement Disorder Society Task Force guidelines. *Mov Disord*. 2012;27:349-356.
16. Boeve BF, Lang AE, Litvan I. Corticobasal degeneration and its relationship to progressive supranuclear palsy and frontotemporal dementia. *Ann Neurol*. 2003;54:S15-S19.
17. Rascovsky K, Hodges JR, Knopman D, et al. Sensitivity of revised diagnostic criteria for the behavioural variant of frontotemporal dementia. *Brain*. 2011;134:2456-2477.
18. Dauvilliers Y, Schenck CH, Postuma RB, et al. REM sleep behaviour disorder. *Nat Rev Dis Primers*. 2018;4:19. doi: 10.1038/s41572-018-0016-5.
19. Hyman BT, Phelps CH, Beach TG, et al. National Institute on Aging- Alzheimer's Association guideline for the neuropathologic assessment of Alzheimer's Disease. *Alzheimers Dement*. 2012;8:1-13.
20. Braak H, Braak E. Neuropathological staging of Alzheimer-related changes. *Acta Neuropathol*. 1991;82:239-259.
21. Mirra SS, Heyman A, McKeel D, et al. The Consortium to establish a registry for Alzheimer's Disease (CERAD). Part II. Standardization of the neuropathologic assessment of Alzheimer's Disease. *Neurology*. 1991;41:479-486.
22. Thal DR, Rub U, Orantes M, Braak H. Phases of A-beta deposition in the human brain and its relevance for the development of AD. *Neurology*. 2002;58:1791-1800.
23. Mackenzie IR, Neumann M, Bigio EH, et al. Nomenclature and nosology for neuropathologic subtypes of frontotemporal lobar degeneration: an update. *Acta Neuropathol*. 2010;119:1-4. doi: 10.1007/s00401-009-0612-2
24. Williams BW, Mack W, Henderson VW. Boston naming test in alzheimer's disease. *Neuropsychologia*. 1989;27:1073-1079.
25. Reisberg B, Ferris SH, de Leon MJ, Crook T. The Global Deterioration Scale for assessment of primary degenerative dementia. *Am J Psychiatry*. 1982;139:1136-1139.

26. Reitan R. Validity of the Trail-Making Test as an indication of organic brain damage. *Percept Mot Skills* 1958;8:271-276.
27. Folstein MF, Folstein SE, McHugh PR. "Mini-mental state". A Practical method for grading the cognitive state of patients for the clinician. *Journal Psychiatr Res.* 1975;12:189-198.
28. Cerhan J, Ivnik RJ, Smith GE, Tangalos EC, Peterson RC, Boeve BF. Diagnostic utility of letter fluency, category fluency, and fluency difference scores in Alzheimer's Disease. *Clin Neuropsychol.* 2002;16:35-42.
29. Sonni I, Ratib O, Boccardi M, et al. Clinical validity of presynaptic dopaminergic imaging with ¹²³I-ioflupane and noradrenergic imaging with ¹²³I-MIBG in the differential diagnosis between Alzheimer's disease and dementia with Lewy bodies in the context of a structured 5-phase development framework. *Neurobio Aging.* 2017;52:228-242.
30. Thomas AJ, Attems J, Colloby SJ, et al. Autopsy validation of ¹²³I-FP-CIT dopaminergic neuroimaging for the diagnosis of DLB. *Neurology.* 2017;88:276-283.
31. Walker Z, Jaros E, Walker RW, et al. Dementia with Lewy bodies: a comparison of clinical diagnosis, FP-CIT single photon emission computed tomography imaging and autopsy. *J Neurol Neurosurg Psychiatry.* 2007;78:1176-1181.
32. Kantarci K, Lowe VJ, B.F. B, et al. Multimodality imaging characteristics of dementia with Lewy bodies. *Neurobiol Aging.* 2012;33:2091-2105.
33. Papathanasiou N, Boutsiadis A, Dickson J, Bomanji JB. Diagnostic accuracy of ¹²³I-FP-CIT (DaTSCAN) in dementia with Lewy bodies: A meta-analysis of published studies. *Parkinsonism Relat Disord.* 2012;18:225-229.
34. Delva A, Van Weehaeghe D, Van Aalst J, et al. Quantification and discriminative power of ¹⁸F-FE-PE2I PET in patients with Parkinson's disease. *Eur J Nucl Med Mol Imaging.* 2019. <https://doi.org/10.1007/s00259-019-04587-y>
35. Jiang Y, Nishikawa RM, Schmidt RA, Toledano AY, Doi K. Potential of computer-aided diagnosis to reduce variability in radiologists' interpretations of mammograms depicting microcalcifications. *Radiology.* 2001;220:787-794.
36. Tang BN, Minoshima S, George J, et al. Diagnosis of suspected Alzheimer's disease is improved by automated analysis of regional cerebral blood flow. *Eur Nucl Med Mol Imaging.* 2004;31:1487-1484.
37. Lange C, Seese A, Schwarzenbock S, et al. CT-Based attenuation correction in I-¹²³-Ioflupane-SPECT. *PLoS One.* 2014;9:e108328.

38. Akahoshi M, Abe K, Uchiyama Y, et al. Attenuation and scatter correction in I-123 FP-CIT SPECT do not affect the clinical diagnosis of dopaminergic system neurodegeneration. *Medicine (Baltimore)*. 2017;96:e8484.
39. Yeo JM, Lim X, Khan Z, Pal S. Systematic review of the diagnostic utility of SPECT imaging in dementia. *Eur Arch Psychiatry Clin Neurosci*. 2013;263:539-552.

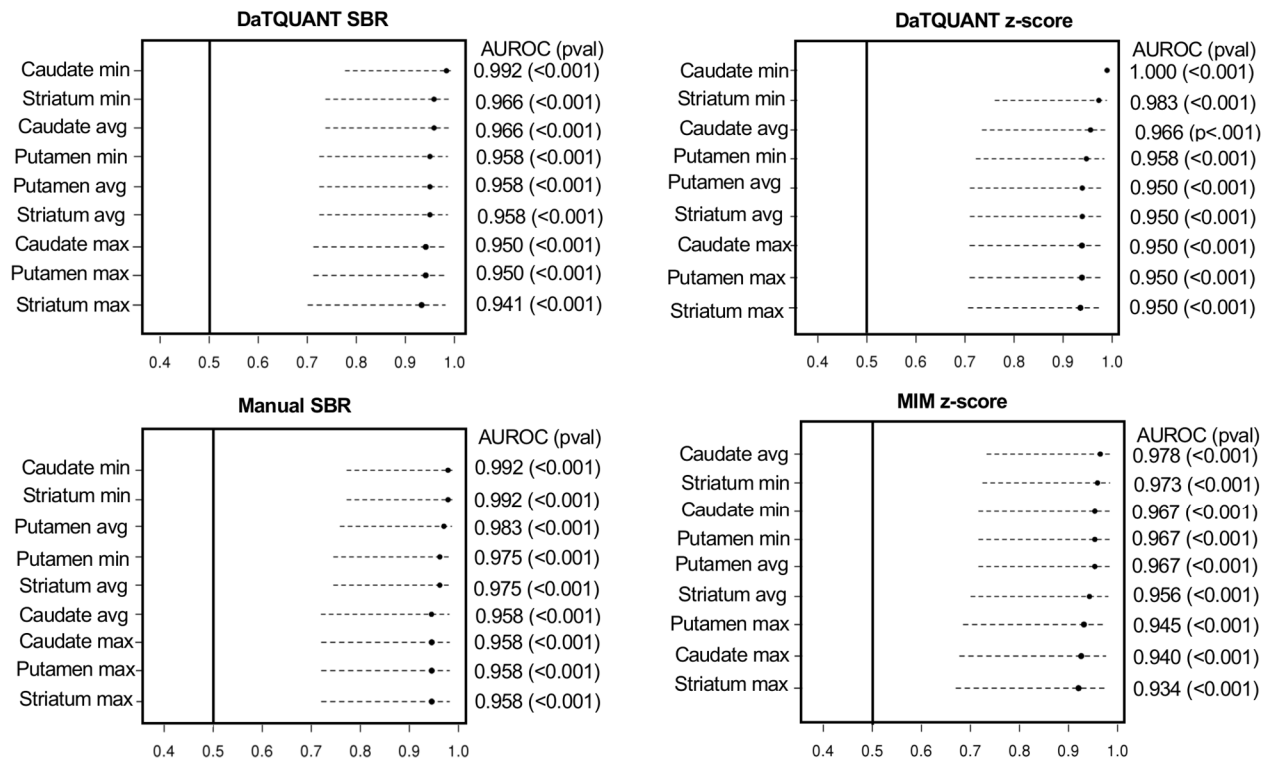


Figure 1. Diagnostic accuracy using area under the receiver operating characteristics (AUROC) of SBR and z-scores for various ROIs as calculated by MIM, DaTQUANT, and manual to differentiate between No-LBD and LBD.

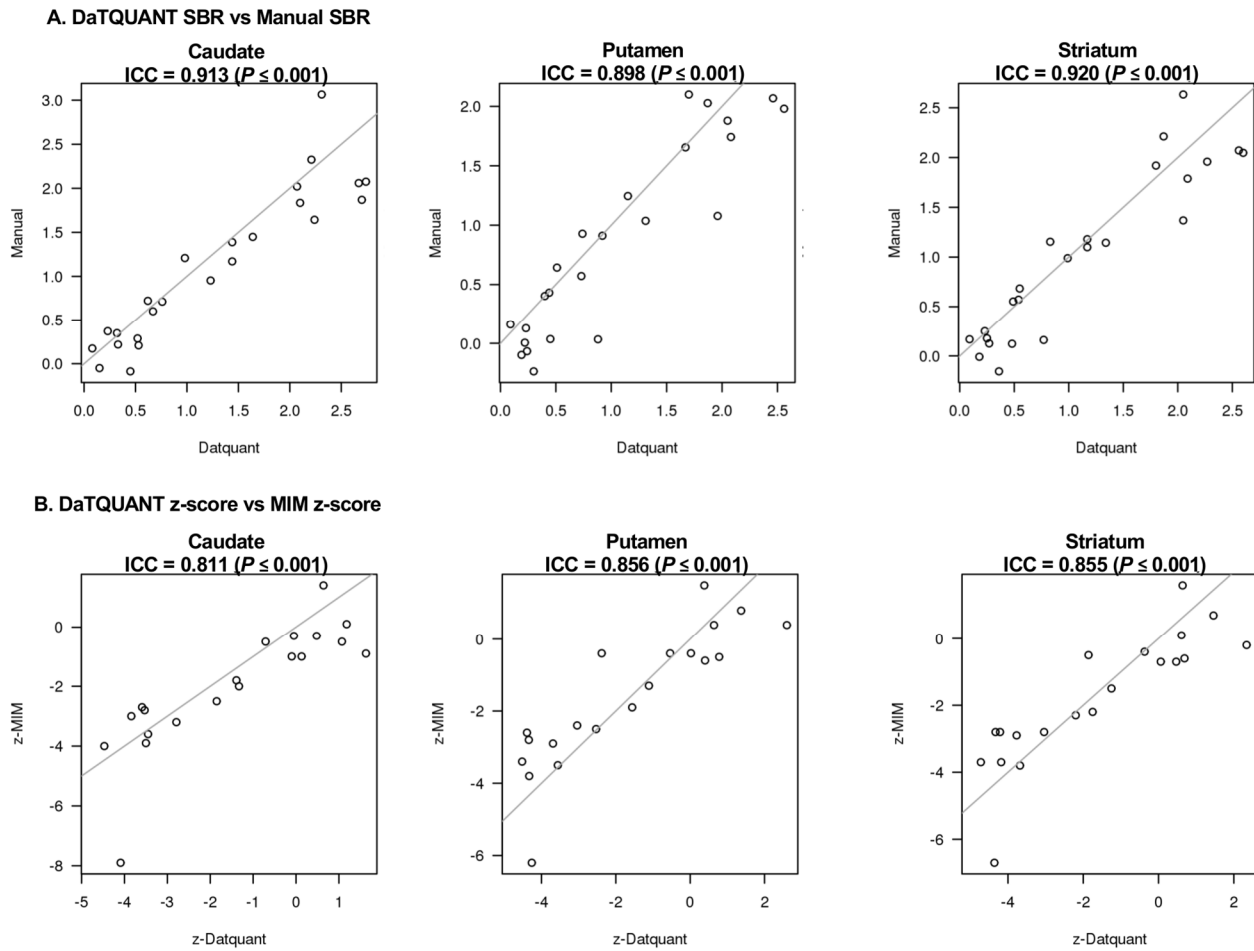


Figure 2. Correlations between programs using minimum caudate, minimum putamen and minimum striatum SBRs and z-scores.

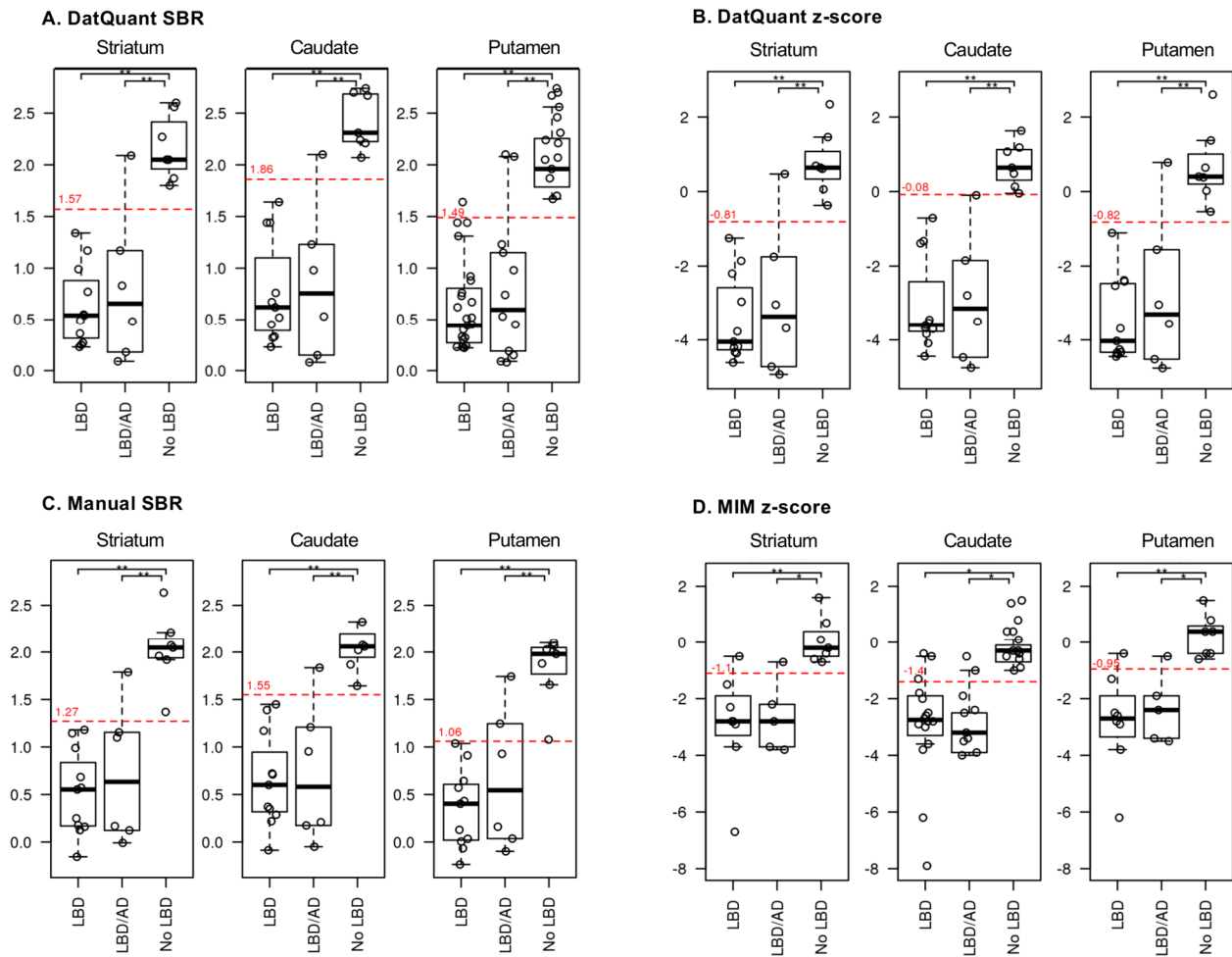


Figure 3. Box-and-whisker plots show the distribution of z-scores and SBRs for the minimum striatum, minimum caudate and minimum putamen amongst LBD, LBD/AD and No-LBD neuropathological diagnoses. Single asterisks represent significance of $0.001 < p < 0.05$, double asterisks represent significance of $p < 0.001$.

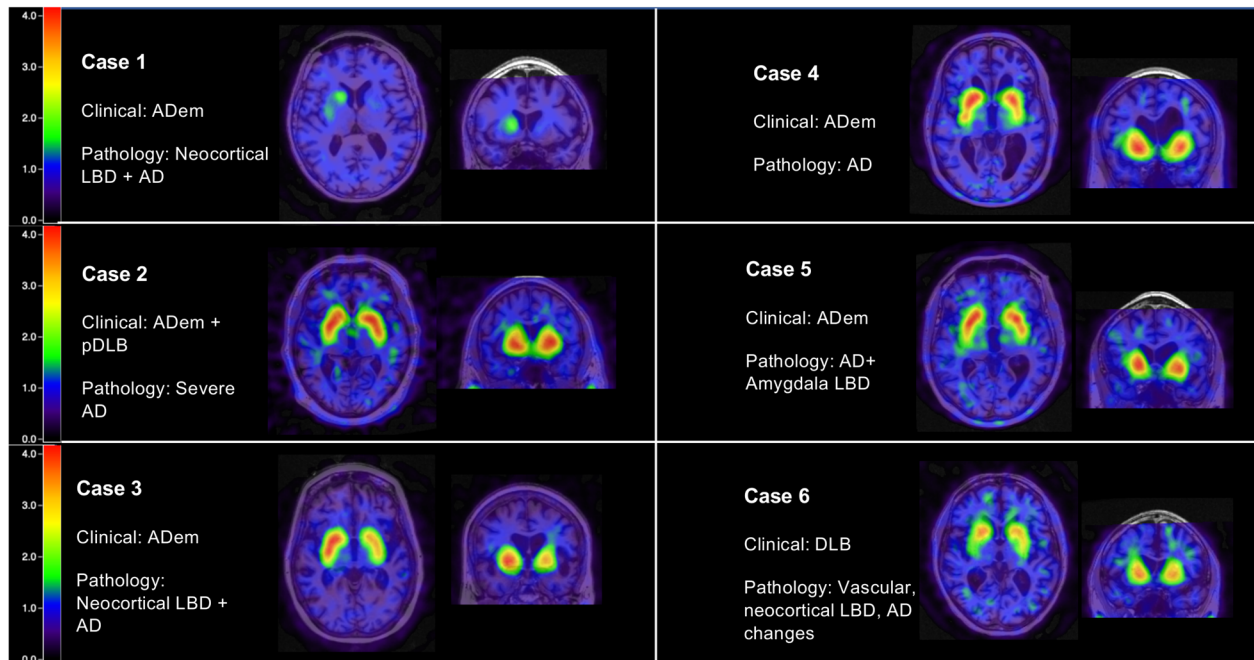


Figure 4. Six cases that underwent ^{123}I -FP-CIT-SPECT and then neuropathology. Clinical diagnoses before death and pathology diagnosis are presented alongside each MRI co-registered images.

Table 1. Clinical data, minimum SBRs, minimum z-scores, ante-mortem and post-mortem diagnosis are shown from six cases that underwent ¹²³I-FP-CIT-SPECT and then neuropathology.

Case No.	Age at Scan	Time Between Last Scan and Death (yrs)	DQ Striatum, SBR(z-score)	DQ Caudate, SBR(z-score)	MIM Striatum, SBR(z-score)	MIM Caudate, SBR(z-score)	Manual Striatum SBR	Manual Caudate SBR	DAT Visual Interpretation	Clinical Diagnosis Before Death	UPDRS	MMSE	CDR® Sum of Boxes
1	75	2.23	0.09 (-4.72)	0.08 (-4.47)	0.27 (-3.70)	0.3 (-4.00)	.17	1.17	Abnormal	ADem	7	N/A	13
2	55	2.06	2.56 (1.46)	2.74 (1.18)	2.77 (0.70)	2.7 (0.10)	2.07	3.08	Normal	ADem + pDLB	5	15	3.5
3	63	2.85	2.09 (0.47)	2.10 (-0.10)	1.98 (-0.70)	2.05 (-1.00)	1.79	2.83	Normal	ADem	0	6	9
4	59	2.93	1.87 (-0.37)	2.21 (-0.05)	2.14 (-0.40)	2.37 (-0.30)	2.21	3.32	Normal	ADem	0	14	6
5	74	4.65	1.80 (0.09)	2.07 (0.20)	1.9 (-0.7)	1.89 (-1.00)	1.92	3.02	Normal	ADem (lpvPPA)	0	20	2
6	77	1.05	1.17 (-1.86)	1.64 (-0.71)	1.99 (-0.5)	2.19 (-0.5)	1.18	2.45	Abnormal	pDLB	11	21	6

Abbreviations: ADem=Alzheimer's disease dementia; CDR® = Clinical Dementia Rating Staging Instrument; DaT=¹²³I-FP-CIT-SPECT; DQ=DaTQUANT, pDLB= Probable Dementia with Lewy bodies, lpvPPA=logopenic variant primary progressive aphasia, MMSE=Mini-mental State Examination, UPDRS=Unified Parkinson's Disease Rating Scale.

Table 2. Clinical and neuropathological data shown from the cases listed in Table 1.

Case	Pathologic diagnosis	Age at death	Sex	Braak	NIA-AA	cDLB-4	Midbrain Lewy body involvement
1	DLBD/AD	78	F	V1	High	Intermediate	Severe-Very Severe
2	AD	57	M	V1	High	None	None
3	DLBD	66	F	V1	Intermediate	Intermediate	Mild
4	AD	62	M	V	Intermediate	None	None
5	AD/ALB	78	M	V1	High	Low	None
6	DLBD/PA/VaD	81	M	II	Low	High	Severe-Very Severe

Abbreviations: AD=Alzheimer's disease; DLBD= Diffuse Lewy Body Disease; AD/ALB=Alzheimer's Disease with amygdala

restricted Lewy Bodies; PA= Pathological Aging; VaD= Vascular Dementia; NIA-AA=National Institute on Aging and Alzheimer's

Disease guidelines; cDLB-4=Fourth Consortium on Dementia with Lewy Bodies.

SUPPLEMENTAL

Supplemental Table 1.

Characteristics table by LBD pathology with the mean (SD) listed for the continuous variables and count (%) for the categorical variables. P-values for differences between groups come from an ANOVA for the continuous variables or a chi-squared test for the categorical variables.

	LBD-Present			LBD-Absent	P-value
	Total	LBD	LBD/AD		
No. of participants	n=17	n=11	n=6	n=7	
DaT Age, yrs (SD)	75.2 (8.8)	77.3 (9.1)	71.3 (7.4)	65.6 (8.0)	0.029*
Male, no. (%)	13 (76%)	10 (91%)	3 (50%)	7 (100%)	0.036*
APOE4, no. (%)	8 (47.1%)	4 (36.4%)	4 (66.7%)	5 (71.4%)	0.27
Age at death, yrs (SD)	78.5 (9.2)	80.5 (9.7)	74.8 (7.5)	68.0 (8.3)	0.028*
Scan to death, yrs (SD)	3.2 (1.9)	3.2 (2.3)	3.3 (0.9)	2.4 (1.6)	0.6
Education, yrs (SD)	15.1 (2.8)	14.9 (2.7)	15.5 (3.2)	16.9 (1.9)	0.33
UPDRS Total	11.8 (7.1)	11.7 (8.4)	12.2 (3.9)	3.4 (6.0)	0.11
MMSE (SD)	20.9 (7.7)	24.5 (4.7)	13.8 (7.9)	15.5 (4.4)	0.003*
CDR® Sum of boxes (SD)	6.3 (4.6)	5.5 (4.7)	8.3 (4.3)	7.5 (4.3)	0.44
Trails A (SD)	84.1 (37.2)	71.4 (33.9)	122.0 (11.5)	84.0 (44.8)	0.14
Dementia Rating Scale Total (SD)	119.8 (16.7)	123.0 (14.6)	110.3 (22.4)	94.7 (20.8)	0.08
Boston Naming Test (SD)	23.0 (6.6)	25.6 (2.8)	18.5 (9.3)	17.6 (7.4)	0.1
Global Deterioration Scale (SD)	4.3 (1.4)	4.1 (1.5)	4.6 (1.1)	5.3 (0.8)	0.22
Category Fluency Total (SD)	21.4 (9.0)	24.9 (4.7)	16.6 (11.7)	11.0 (4.5)	0.03*
pDLB, no. (%)	12 (71%)	8 (73%)	4 (67%)	0 (0%)	
ADem no. (%)	2 (12%)	0 (0%)	2 (33%)	5 (71%)	
Other, no. (%)	3 (18%)	3 (27%)	0 (0%)	2 (29%)	

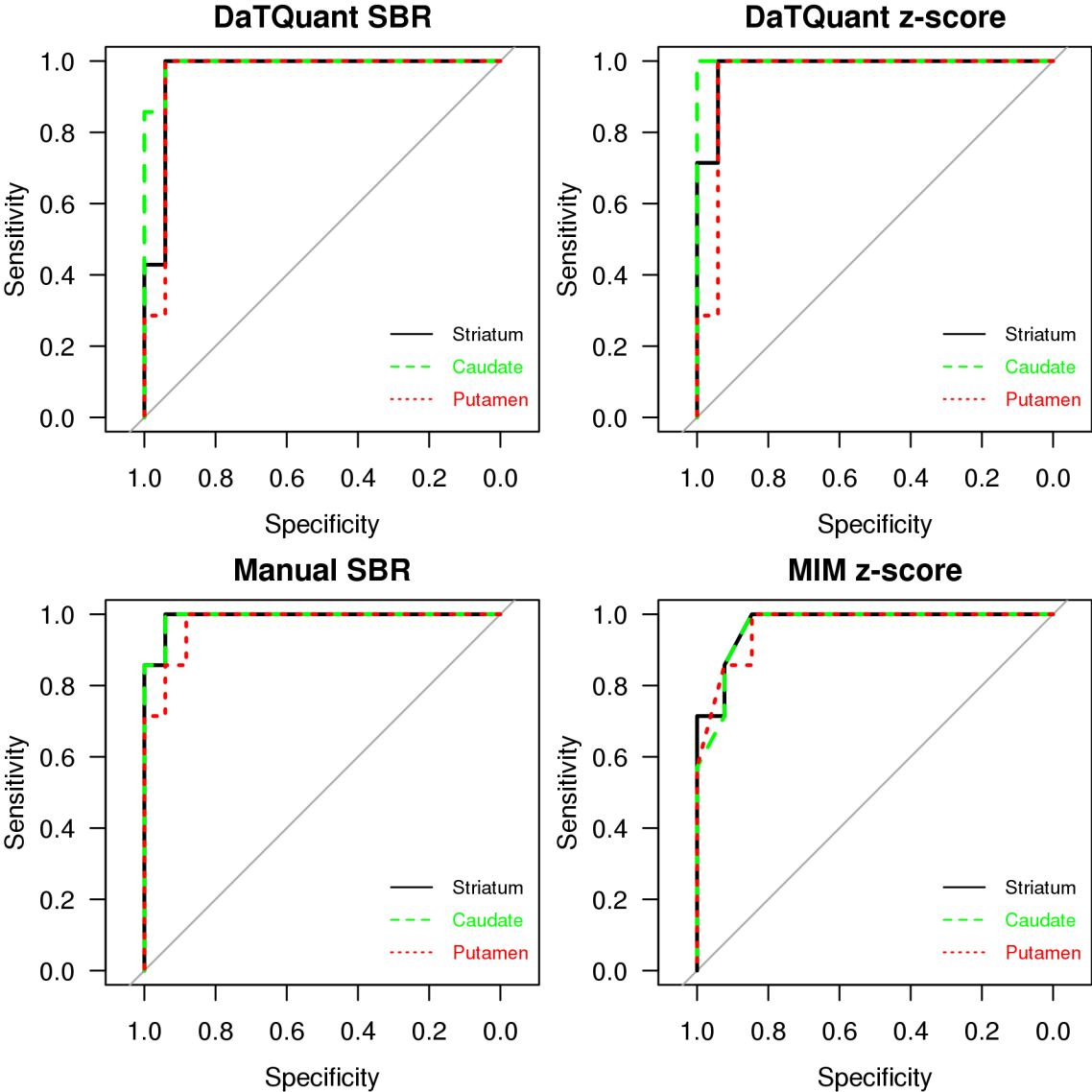
Abbreviations: AD=Alzheimer's disease; ADem=Alzheimer's disease dementia;

APOE4=Apolipoprotein ε4; CDR® = Clinical Dementia Rating Staging Instrument; DaT=¹²³I-

FP-CIT SPECT; pDLB= Probable Dementia with Lewy bodies; LBD=Lewy body disease;

MMSE=Mini-mental State Examination; UPDRS=Unified Parkinson's Disease Rating Scale.

Supplemental Figure 1. 2x2 AUROC figures for each semi-quantitative program: DaTQuant, MIMneuro and Manual. Each program has excellent discrimination between LBD and Non-LBD across the minimum striatum, minimum caudate and minimum putamen.



Supplemental Table 2. Proposed cutoff values showcased on the box-and-whisker plots shown in Figure 4, derived from the Youden method.

	Proposed Cutoff Value
DaTQUANT	
Striatum	1.57
Caudate	1.86
Putamen	1.49
zDaTQUANT	
Striatum	-.81
Caudate	-.08
Putamen	-.82
Manual	
Striatum	1.27
Caudate	1.55
Putamen	1.06
zMIM	
Striatum	-1.1
Caudate	-1.4
Putamen	-.95

Supplemental Table 3. Table of p-values from an ANOVA with contrast statements for the pairwise comparison.

	AD vs LBD	AD vs LBD/AD	LBD vs LBD/AD
DaTQUANT			
Striatum	<0.001	<0.001	0.49
Caudate	<0.001	<0.001	0.77
Putamen	<0.001	<0.001	0.37
zDaTQUANT			
Striatum	<0.001	<0.001	0.49
Caudate	<0.001	<0.001	0.81
Putamen	<0.001	<0.001	0.36
Manual			
Striatum	<0.001	<0.001	0.44
Caudate	<0.001	<0.001	0.81
Putamen	<0.001	<0.001	0.23
zMIM			
Striatum	<0.001	0.004	0.75
Caudate	0.003	0.01	0.9
Putamen	<0.001	0.004	0.54